Neoplasia 49 (2024) 100965

Contents lists available at ScienceDirect

Neoplasia

journal homepage: www.elsevier.com/locate/neo

DNA methylation landscape reveals *GNAS* as a decitabine-responsive marker in patients with acute myeloid leukemia

Shujiao He [a], Yan Li [b,c], Lei Wang [a], Yisheng Li [d,e], Lu Xu [a], Diya Cai [a], Jingfeng Zhou [a,*], Li Yu [a,*]

[a] *Department of Hematology and Oncology, International Cancer Center, Shenzhen Key Laboratory, Hematology Institution of Shenzhen University, Shenzhen University General Hospital, Shenzhen University Health Science Center, Shenzhen University, Xueyuan Ave 1098, Nanshan District, Shenzhen 518000, China*
[b] *Department of Hematology, Peking Third Hospital, 49 North Garden Road, Beijing 100191, China*
[c] *Department of Haematology, Chinese People's Liberation Army General Hospital, Beijing 100853, China*
[d] *Shenzhen Haoshi Biotechnology Co., Ltd, 155 Hong Tian Rd, Baoan District, Shenzhen 518125, China*
[e] *Shenzhen University-Haoshi Cell Therapy Institute, 155 Hong Tian Rd, Baoan District, Shenzhen 518125, China*

ARTICLE INFO

Keywords:
Acute myeloid leukemia
Prognostic biomarker
Decitabine
Differentially methylated region
DNA methylation sequencing
GNAS

ABSTRACT

Background: The demethylation agent decitabine (DAC) is a pivotal non-intensive alternative treatment for acute myeloid leukemia (AML). However, patient responses to DAC are highly variable, and predictive biomarkers are warranted. Herein, the DNA methylation landscape of patients treated with a DAC-based combination regimen was compared with that of patients treated with standard chemotherapy to develop a molecular approach for predicting clinical response to DAC.
Methods: Twenty-five non-M3 AML patients were enrolled and subjected to DNA methylation sequencing and profiling to identify differentially methylated regions (DMRs) and genes of interest. Moreover, the effects of a DAC-based regimen on apoptosis and gene expression were explored using Kasumi-1 and K562 cells.
Results: Overall, we identified 541 DMRs that were specifically responsive to DAC, among which 172 DMRs showed hypomethylation patterns upon treatment and were aligned with the promoter regions of 182 genes. In particular, *GNAS* was identified as a critical DAC-responsive gene, with *in vitro GNAS* downregulation leading to reduced cell apoptosis induced by DAC and cytarabine combo treatment.
Conclusions: We found that *GNAS* is a DAC-sensitive gene in AML and may serve as a prognostic biomarker to assess the responsiveness of patients with AML to DAC-based therapy.

Background

Gain and loss of DNA methylation profoundly influence the pathogenesis of acute myeloid leukemia (AML) [1,2]. Indeed, it is well established that DNA methylation-mediated silencing of tumor suppressor genes, which typically occurs in promoter regions, contributes to leukemogenesis and progression of AML [3]. The methylation landscape of AML is frequently disrupted and characterized by global hypomethylation accompanied by local hypermethylation [4]. In contrast, healthy individuals exhibit a DNA methylation profile with bimodal patterns, in which the genome is predominantly hypermethylated with unmethylated CpG islands [5]. Hence, given the reversibility of DNA methylation, hypomethylating agents are widely used in AML to restore normal methylation landscapes [6,7].

Although standard intensive chemotherapy remains the first-line treatment for AML, patients with poor performance status or comorbidities are not always eligible due to increased treatment-related morbidity and mortality [8]. Nonetheless, decitabine (DAC), a well-known hypomethylating agent, has been widely used for the treatment of these patients [6]. Low-dose DAC exerts antineoplastic effects on AML cells by restoring their DNA methylation profile, with DAC monotherapy achieving a response rate within 14–47% in newly diagnosed patients [9–11], and leading to an impressive remission rate of 16–43% [12,13] in patients with relapsed/refractory AML when used in combination with low-dose cytarabine (Ara-C). As indicated by the wide range of response rates, many patients remain resistant to DAC. Hence,

Abbreviations: AML, acute myeloid leukemia; Ara-C, cytarabine; CR, complete remission; DAC, decitabine; DCAG, decitabine, cytarabine, aclarubicin, and granulocyte colony-stimulating factor; DMR, differentially methylated region; DNMT, DNA methyltransferase; PCR, polymerase chain reaction; qRT-PCR, quantitative real-time PCR; shRNA, short hairpin RNA; TSS, transcription start site.

* Corresponding authors.
E-mail addresses: Jingfengzhou@szu.edu.cn (J. Zhou), yuli@szu.edu.cn (L. Yu).

https://doi.org/10.1016/j.neo.2024.100965
Received 27 July 2023; Received in revised form 31 December 2023; Accepted 2 January 2024

predictive biomarkers for DAC response are urgently needed to enable personalized drug selection. Herein, we aimed to identify DAC-sensitive methylation regions and genes in patients with AML.

Materials and methods

Patients

Between August 2014 and June 2016, 25 non-M3 AML patients who visited the hematology department of the Chinese People's Liberation Army General Hospital were enrolled and underwent DNA methylation sequencing as previously described [14]. A methylation sequencing dataset containing data from 32 bone marrow samples, including 18 non-paired *de novo* samples and 7 paired *de novo*/complete remission (CR) samples, was obtained. *De novo* samples were obtained before treatment. All CR samples were obtained after the first round of treatment and included two samples derived from patients who received standard chemotherapy (Ara-C for 7 days and idarubicin for 3 days) and five samples derived from patients who received the decitabine, Ara-C, aclarubicin, and G-CSF (DCAG) regimen (decitabine 20 mg/m^2 d1–5; Ara-C 10 mg/m^2 q12h d1–5; aclarubicin 20 mg d1, d3, d5; and G-CSF 300 μg/d from d0 to neutrophil recovery). All patients were diagnosed and evaluated according to the World Health Organization 2016 classification and the AML guidelines of the National Comprehensive Cancer Network (Version 1.2017; http://www.nccn.org/). Written informed consent was obtained from each participant prior to specimen collection, as previously described [14]. Patient characteristics are summarized in Tables 1 and 2.

DNA methylation sequencing

Bone marrow samples were subjected to Ficoll density gradient separation (Sigma-Aldrich, St. Louis, MO, USA) to enrich for mononuclear cells, followed by DNA purification using the Wizard Genomic DNA Purification Kit (Promega, Madison, WI, USA). MethylC-capture sequencing was performed as previously described [14]. Briefly, bisulfate-converted DNA fragments were amplified, a sequencing library was constructed using the SeqCap Epi enrichment system (Roche NimbleGen, Madison, WI, USA), and the DNA was sequenced using a HiSeq2500 system (Illumina, San Diego, CA, USA).

Methylation profiling

Raw sequencing data were analyzed using Bismark [15] (v0.10.1; parameters: -pe, -bowtie2, -directional, -unmapped) to map methylation regions to the GRCh37 human assembly genome following the removal of adapter sequences and poor-quality reads. The methylation level at each site was calculated by dividing the number of methylated reads by the total number of reads covered. Differentially methylated regions (DMRs) were identified using Metilene [16] (v0.2-6; parameters: -M 300, -m 5, -d 0.2, -f 1, -t 1). DMRs exhibiting changed of $\geq$ 20% were subjected to sequential analysis. Recurrent or unique DMRs between different treatment groups were identified using Bedtools (v2.25.0, https://bedtools.readthedocs.io/en/latest/; parameters: intersect -a DMRa.bed, -b DMRb.bed, -wa). Regions within −2 200 and 500 bp of transcription start sites (TSS) were marked as "Promoter," those overlapping the gene body were marked as "Gene body," regions partially overlapping the promoter and the gene body were marked as "Span TSS, " and the remaining regions were marked as "Other."

Table 2
Characteristic of de novo samples (n = 18).

Characteristic	Value
Age at diagnosis, years	50.06 ± 13.67
Sex, No. (%)	
Male	9 (50.00)
Female	9 (50.00)
Bone marrow blast, No. (%)	69.94 ± 25.14
AML FAB subtype, No. (%)	
M1	1 (5.56)
M2	2 (11.11)
M4	6 (33.33)
M5	8 (44.44)
M6	1 (5.56)
2017 NCCN Cytogenetic risk classification, No. (%)	
Good	1 (5.56)
Intermediate	16 (88.89)
Poor	1 (5.56)
2017 NCCN Molecular risk classification, No. (%)	
Good	1 (5.56)
Intermediate	16 (88.89)
Poor	1 (5.56)

Gene set enrichment analysis

Gene Ontology (GO), Kyoto Encyclopedia of Genes and Genomes (KEGG), and Reactome gene set enrichment analyses were conducted using Metascape (https://metascape.org/gp/index.html#/main/step1) with a *p*-value cutoff of 0.01.

Cell culture and treatment

Kasumi-1 and K562 cell lines (American Type Culture Collection, Manassas, VA, USA) were maintained in RPMI 1640 medium (Gibco, Thermo Fisher Scientific, Waltham, MA, USA) containing streptomycin (100 μg/ml), penicillin (50 U/ml), and 10% fetal bovine serum (all from Gibco). The cells were stored in plastic tissue culture plates in a 5% CO_2 humidified atmosphere at 37 °C. Lyophilized DAC and Ara-C (Topscience, Shanghai, China) were dissolved in dimethyl sulfoxide (Thermo Fisher Scientific) and stored at −80 °C.

Lentivirus packaging and infection

Human embryonic kidney 293T cells (ATCC) were cultured in Dulbecco's modified Eagle's medium supplemented with streptomycin (100 μg/ml), penicillin (50 U/ml), and 10% fetal bovine serum. Short hairpin RNAs (shRNA; Sigma-Aldrich) were cotransfected into 293T cells along with pHR and VSVG plasmids to produce shRNA lentiviruses. Kasumi-1 and K562 cells were transfected with shRNA lentiviruses targeting *GNAS* (shGNAS) or a negative control (shNC).

Table 1
Characteristic of *de novo*/CR paired samples (n = 7).

	Age (years)	Sex	Bone marrow blast at diagnosis %	AML FAB subtype	Risk classification	Induction regimen
paire1	59	Female	45.2	M5	Poor	DCAG
paire2	21	Female	57.6	M4	Good	7+3
paire3	34	Female	67.2	M4	Good	DCAG
paire4	60	Female	56.4	M4	Intermediate	DCAG
paire5	73	Female	81	M2	Good	DCAG
paire6	50	Female	83.2	M2	Good	DCAG
paire7	26	Male	91.2	M5	Poor	7+3

CR: complete remission

Apoptosis assay

Cells transfected with the shNC or shGNAS lentiviruses were treated with 10 nM DAC for 3 days, after which the medium was replaced. On day 4, 2×10^5 cells per well were seeded onto 6-well plates and either left untreated or treated with 100 nM Ara-C for 3 days. After treatment, the cells were harvested and stained with annexin V-FITC (BD, Franklin Lakes, NJ, USA) for 15 min at room temperature in the dark. Propidium iodide was added to distinguish between living and dead cells, and the apoptosis rate was analyzed using a CytExpert flow cytometer (Beckman Coulter Life Sciences, Indianapolis, IN, USA). Apoptosis was assayed in triplicate under the following experimental conditions: DAC alone, Ara-C alone, and DAC followed by Ara-C.

DNA extraction and methylation-specific polymerase chain reaction (PCR)

Genomic DNA from Kasumi-1 and K562 cells was isolated using the Wizard Genomic DNA Purification Kit (Promega). Genomic DNA was treated with sodium bisulfate (EpiTect Bisulfite Kit; Qiagen, Hilden, Germany) according to the manufacturer's instructions. Methylation-specific PCR primer sequences were designed using MethPrimer (http://www.urogene.org/methprimer/) and are listed in Supplementary Table S1. Methylation-specific PCR was conducted in a 25 μl reaction solution using GoTaq Green Master Mix (Promega). PCR products were analyzed by electrophoresis with a 2% agarose gel.

RNA extraction and quantitative PCR

TRIzol reagent (Invitrogen, Thermo Fisher Scientific) was used to extract total RNA, which was used to synthesize cDNA (Takara Bio Inc., Kusatsu, Japan). Quantitative real-time PCR (qRT-PCR) was conducted using an ABI PRISM 7500 Sequence Detection System (Applied Biosystems, Thermo Fisher Scientific) with the following conditions: 95°C for 30 s to denature the cDNA template, followed by 40 cycles of 95°C for 5 s and 60°C for 20 s. Gene levels were determined using the $2^{-\Delta\Delta Ct}$ method. The primers used for qRT-PCR are listed in Supplementary Table S2. Independent experiments were performed in triplicate.

Western blotting

Cells were lysed in radioimmunoprecipitation assay buffer supplemented with phenylmethylsulfonyl fluoride and phosphatase inhibitors (Roche, Basel, Switzerland). Protein concentration was determined using a BCA protein assay kit (Thermo Fisher Scientific). Proteins were subjected to sodium dodecyl-sulfate polyacrylamide gel electrophoresis and transferred to polyvinylidene fluoride membranes. The membranes were probed with the following primary antibodies: anti-GNAS (1:1000, ab283266; Abcam, Cambridge, UK), anti-DNMT3A (1:1000, ab188470; Abcam), and anti-GAPDH (RM2002; Beijing Ray Antibody Biotech, Beijing, China). Goat radish peroxidase-linked anti-rabbit IgG (31463) and goat radish peroxidase-linked anti-mouse IgG (31437) were purchased from Invitrogen.

Statistical analysis

SPSS software (version 20.0; IBM Corp, Armonk, NY, USA) was used for statistical analyses. All data are expressed as mean ± standard error of at least three independent experiments. Student's *t*-test and one-way analysis of variance were used to determine statistical differences among experimental groups. All statistical tests were two-sided, and statistical significance was defined as $p < 0.05$.

Results

Identification of DAC-sensitive DMRs in paired samples

To determine the effects of the DCAG regimen and conventional chemotherapy on the methylation landscape of AML patients (Fig. 1), we initially evaluated and compared the methylation patterns of five sets of *de novo*/CR-paired samples from patients administrated the DCAG regimen (Table 1). Recurrent DMRs with the same change direction across all paired samples were collectively named the "DMR1" profile and were selected for further analysis (Fig. 2a). As expected, no recurrent DMRs with opposite change directions were observed among these paired samples. Hypermethylated DMR1 with reduced methylation levels after treatment (n = 2 455, 98.44%) accounted for the majority of DMRs within the DMR1 profile (Fig. 2b). The genomic distribution of DMR1 was preferentially enriched at gene body regions, with 53.20% and 46.15% of hyper- and hypomethylation patterns, respectively. In contrast, 36.82% and 7.69% of hyper- and hypomethylated DMR1, respectively, were mapped to promoter regions (Fig. 2c).

We also compared the methylation signatures of two sets of *de novo*/CR-paired samples from patients treated with the "7 + 3" standard chemotherapy regimen (Table 1). Recurrent DMRs with the same change direction between the two sets of paired samples were collectively named "DMR2" profile (Fig. 2d). DMR2 contained significantly more hypomethylated DMRs with increased methylation levels after treatment (n = 1 942) than DMR1 (n = 39) (Fig. 2e). Hypermethylated DMRs with decreased methylation levels after treatment accounted for 98.44% of DMR1 (Fig. 2b) and only 55.16% of DMR2 (Fig. 2e). Although conventional chemotherapy altered the methylation profiles of AML patients, the DCAG regimen exerted a more significant demethylation effect. DMR2 was more enriched in DMRs affecting non-promoter regions than promoter regions (Fig. 2f).

To reduce the influence of unspecific DNA methylation changes caused by traditional chemotherapy, we aligned DMR2 with DMR1 (Fig. 2g). DMRs comprised only in DMR1 (Unique DMR1; Fig. 2g–i) and overlapping DMRs with opposite change directions between DMR1 and DMR2 (Fig. 2g, j, k) were considered DAC-responsive DMRs (hereafter named the "DMR3" profile). DMR3 consisted of 1 946 hypermethylated regions and 30 hypomethylated regions that lost and gained methylation after treatment, respectively (Fig. 2h, k). Gene body regions were the most affected across the genome (Fig. 2i, k), containing 53.24% and 55.17% of hyper- and hypomethylated DMRs within DMR3, respectively.

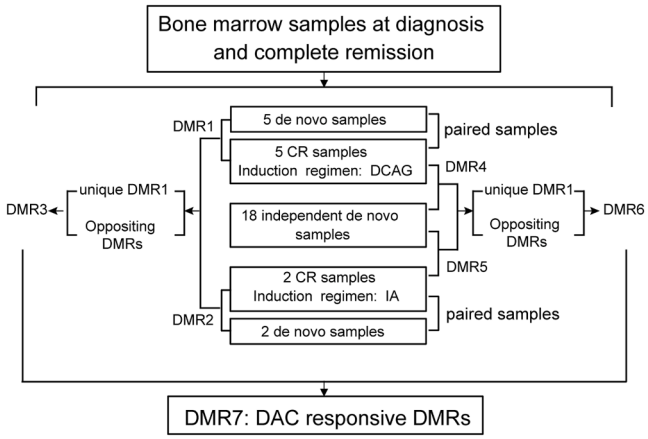

Fig. 1. Study flow chart. Overview of the study cohort and follow-up analyses to identify decitabine (DAC)-responsive regions.

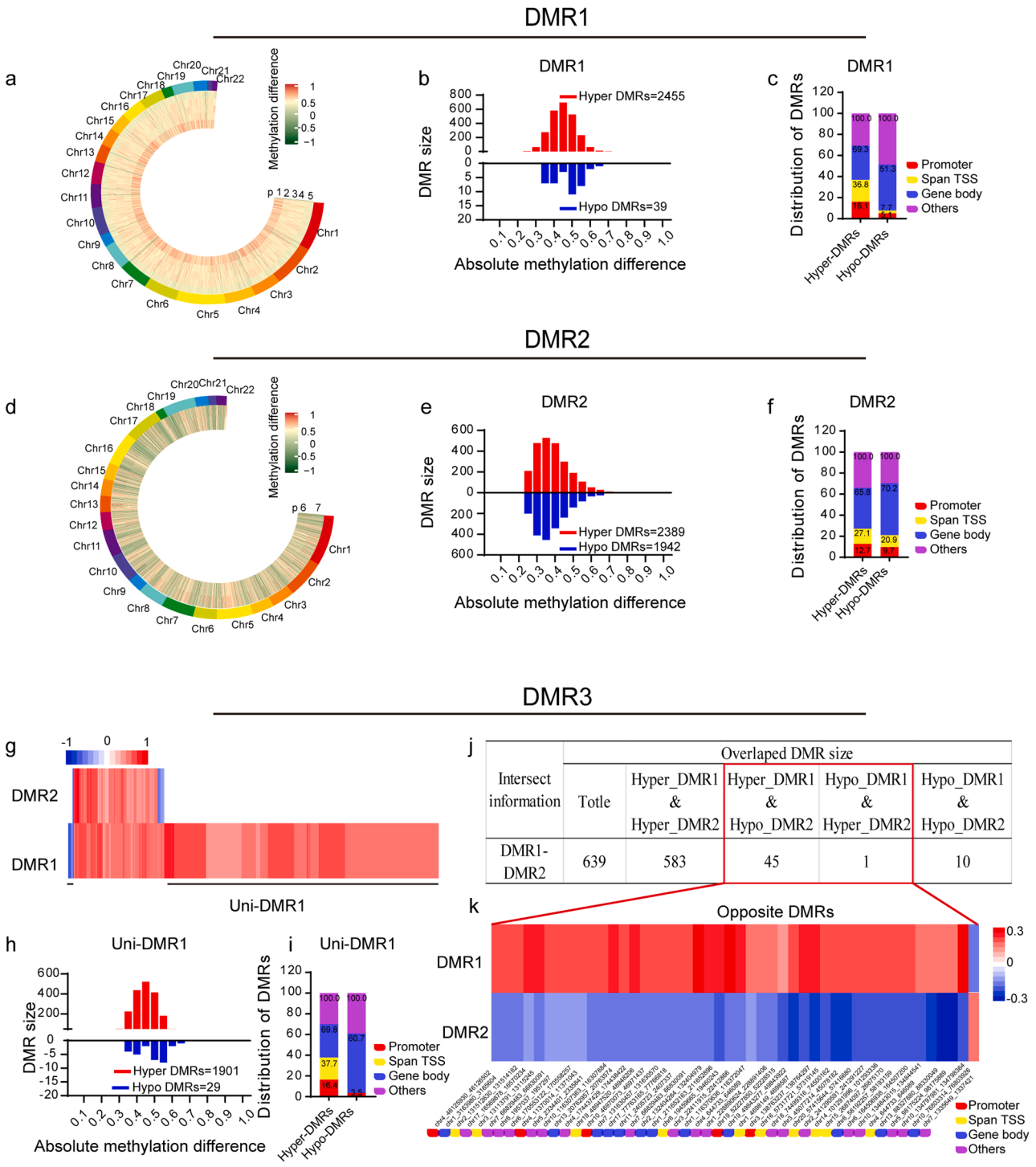

Intersect information	Overlaped DMR size				
	Totle	Hyper_DMR1 & Hyper_DMR2	Hyper_DMR1 & Hypo_DMR2	Hypo_DMR1 & Hyper_DMR2	Hypo_DMR1 & Hypo_DMR2
DMR1-DMR2	639	583	45	1	10

Fig. 2. Characterization of DMR1–DMR3. a Recurrent DMRs (DMR1) in five sets of *de novo*/CR-paired samples across the euchromosome. CR samples were obtained after one cycle of induction chemotherapy with the DCAG regimen. **b** Following treatment, 2 455 former hypermethylated regions in the five *de novo* samples (hyper-DMR1) exhibited a significant reduction in the methylation level (absolute methylation difference > 0.2), and 39 former hypo-DMR1 regions exhibited significantly upregulated methylation levels. **c** Genomic distribution of DMR1. More DMRs were mapped to gene body than promoter regions, and more hyper-DMRs were mapped to promoter regions than were hypo-DMRs. **d** Alignment of recurrent DMRs (DMR2) in two sets of *de novo*/CR-paired samples across the euchromosome. CR samples were obtained after one cycle of treatment with standard chemotherapy. **e** Following treatment, 2 389 former hypermethylated regions in the two *de novo* samples exhibited a significant reduction in methylation levels, and 1 942 former hypomethylated regions exhibited significantly upregulated methylation levels. **f** Genomic distribution of DMR2. DMRs were much more abundant in non-promoter than in promoter regions. **g** Alignment of DMR2 with DMR1. Unique DMR1 regions and overlapping DMRs with opposite change directions were included in DMR3. **h** A total of 1 930 unique DMR1 regions were identified, among which 1 901 DMRs exhibited decreased methylation levels after treatment, whereas only 29 DMRs exhibited elevated methylation levels. **i** Genomic distribution of unique DMR1 regions. **j** Table presenting the 639 overlapping DMRs between DMR1 and DMR2. **k** Heatmap illustrating the 46 overlapping DMRs with opposite change directions. DMR, differentially methylated region; DCAG, decitabine, cytarabine, aclarubicin, and G-CSF; CR, complete response; DAC, decitabine.

Identification of DAC-sensitive DMRs in independent samples

To further refine the set of DAC-responsive DMRs, we compared the methylation alteration patterns of five DCAG-induced CR samples with those of 18 independent *de novo* AML samples (Table 2). A total of 26 581 DMRs were identified, hereafter collectively named "DMR4." After exposure to DCAG treatment, 24 946 (93.85%) hypermethylated regions and 1 635 (6.15%) hypomethylated regions exhibited significantly decreased and increased methylation levels, respectively (Fig. 3a). Further investigation on the genomic location of these DMRs revealed that both hyper- and hypomethylated DMRs were common in DMR4, and were predominantly located in gene body regions (*i.e.*, in the Gene body [53.92%] and Span TSS [60.61%]), whereas the proportion of hypermethylated DMRs that mapped to the promoter region (*i.e.*, in the Promoter region and Span TSS) was much greater (32.44%) than the proportion of hypomethylated DMRs (12.91%) (Fig. 3b).

To eliminate the effect of non-specific methylation changes caused by chemotherapy, we compared the methylation status of 18 independent *de novo* samples with those of two CR samples from patients treated with standard chemotherapy. In total, 27 418 DMRs were identified and were collectively named "DMR5." Consistent with the effects of the DCAG regimen, the number of DMRs with decreased methylation after treatment (24 888, 90.77%) was much greater than that of DMRs with increased methylation (2 530, 9.23%; Fig. 3c). As shown on the DMR5 localization map (Fig. 3d), gene bodies were predominantly affected by both hyper- (14 096, 56.64%) and hypomethylated (1 531, 60.54%) DMRs, whereas promoter regions contained 7 985 (32.08%) hyper- and 419 (16.67%) hypomethylated DMRs.

As performed previously, we next aligned the DMR5 with DMR4 profiles, using DMR4 as the reference DNA set, to identify shared and unique DMRs (Fig. 3e). Recurrent DMRs with the same change direction between DMR4 and DMR5 were considered non-specific methylation changes induced by chemotherapy, whereas recurrent DMRs with opposite change directions between the profiles (Fig. 3f) and DMRs unique to DMR4 (Fig. 3e) were considered DAC-responsive DMRs, being collectively named "DMR6." In total, 9 191 unique DMRs, including 8 506 (93.13%) hypermethylated and 613 (6.87%) hypomethylated DMRs were identified (Fig. 3g, h), along with 13 (12.31%) hypermethylated and one (7.69%) hypomethylated opposite DMRs (Fig. 3i). As expected, after DAC treatment, DMRs predominantly exhibited decreased methylation levels (93.32%). In addition, DMR6 patterns primarily localized on gene body regions (57.59%).

Identification of DAC-sensitive DMRs and genes

To effectively identify DAC-responsive DMRs in patients with AML, we compared the methylation profiles of DAC-sensitive DMRs in paired samples (DMR3) with those in independent samples (DMR6) (Fig. 3j). Consequently, 541 overlapping DMRs with the same change direction were identified and collectively named "DMR7" (Fig. 3j). DMR7 contained 538 (99.45%) DMRs that exhibited decreased methylation levels after treatment (Fig. 3k). Among these, 172 (27.04%) aligned with the promoter regions of 187 genes (Fig. 3l); the gene list is available in Supplementary Table S3. One of the three hypomethylated DMRs in DMR7 localized on a gene body and the other two mapped on intergenic regions.

Considering the established methylation-induced silencing effect on promoter regions, we preferentially examined DMRs located on promoters. Subsequently, the 187 mapped genes were subjected to enrichment analysis to identify genes of interest and evaluate the potential mechanism of demethylation therapy. In particular, *GNAS* was found to be simultaneously involved in several active pathways according to gene ontology (Fig. 4a), KEGG (Fig. 4b), and Reactome (Fig. 4c) enrichment analyses. Therefore, *GNAS* was identified as a DAC-sensitive gene and was examined further.

Effect of DAC on GNAS expression

To determine whether *GNAS* could serve as a predictor of patient response to DAC treatment, we conducted an *in vitro* study to explore the relationship between DAC and *GNAS*. First, we examined whether DAC affected *GNAS* expression in Kasumi-1 and K562 cell lines. Noteworthily, *GNAS* expression was significantly elevated upon treatment with 10 nM DAC (Fig. 4d), as well as its protein levels (Fig. 4e, f), whereas DNMT3A levels were decreased, as expected (Fig. 4e, f). These results suggested that treatment with DAC promotes the expression of *GNAS*.

To further elucidate the mechanism of DAC-mediated *GNAS* upregulation, we retrieved the DMR sequence that mapped to the *GNAS* promoter region for methylation-specific PCR analysis. We found that the two small regions within *GNAS* DMR were methylated in the Kasumi-1 and K562 cell lines (Fig. 4g). Hence, through the demethylation of the two DNA sequence, DAC managed to activate the expression of GNAS.

Effect of GNAS downregulation on cell death induced by DAC/Ara-C combo therapy

To investigate the role of *GNAS* in AML, we knocked down *GNAS* in Kasumi-1 and K562 cell lines using shRNA-carrying lentiviruses. *GNAS* downregulation was initially verified by qRT-PCR (Fig. 4h). Next, we use western blotting to examined GNAS levels in three conditions: cells treated with DAC, cells transfected with the shGNAS, and cells transfected with the shGNAS and treated with DAC (Fig. 4i, j). We confirmed that the upregulation of *GNAS* by DAC was counteracted by the presence of shGNAS in both cell lines.

The sequential combination of DAC and Ara-C is known to have a synergistic effect in AML cells [17]. Thus, we conducted an apoptosis assay using *GNAS*-knocked down cells sequentially treated with DAC and Ara-C (Fig. 5a–d). Consistent with the previous study, Kasumi-1 and K562 cells pre-sensitized with DAC were much more vulnerable to Ara-C, where *GNAS* knockdown counteracted the synergistic killing effect of DAC and Ara-C. Thus, these findings suggested that GNAS mediates the pre-sensitization effect of DAC on AML cells.

Relationship between YAP and GNAS expression

YAP plays a critical role in the pathogenesis of malignancies and it was recently shown to mediate resistance to chemotherapy in AML cells [18,19]. *YAP* is associated with cell growth and adhesion, lipogenesis, and numerous G-protein–coupled receptor ligands [19]. Notably, these characteristics are associated with the enriched signaling pathway we identified as being related to *GNAS* role in AML (Fig. 5a–c; marked with black arrow). Therefore, it is reasonable to speculate that *GNAS* and *YAP* could be molecular partners in AML. To test this hypothesis, we first examined the expression of *YAP* in cells treated with DAC. DAC treatment induced the expression of *YAP* and *CCN2*, an identified target gene of YAP, in Kasumi-1 and K562 cells (Fig. 5e, f). To confirm that the upregulation of *YAP* and *CCN2* was mediated by *GNAS*, we evaluated the expression of *YAP* in cells transfected with shGNAS and found that *YAP* and *CCN2* were downregulated upon *GNAS* knockdown (Fig. 5g–j). Thus, we confirmed that *YAP* partakes the *GNAS*-mediated DAC sensitization effect.

Discussion

For newly diagnosed patients with AML who cannot tolerate intensive chemotherapy, a low-intensity regimen involving hypomethylating agent-based combination regimens is recommended. DAC is one of the most frequently used hypomethylating agents in clinical practice [12]. However, given the variability in patient response to DAC, predictive biomarkers are urgently needed. For decades, investigators have explored the molecular mechanisms of DAC. Although DAC exerts a

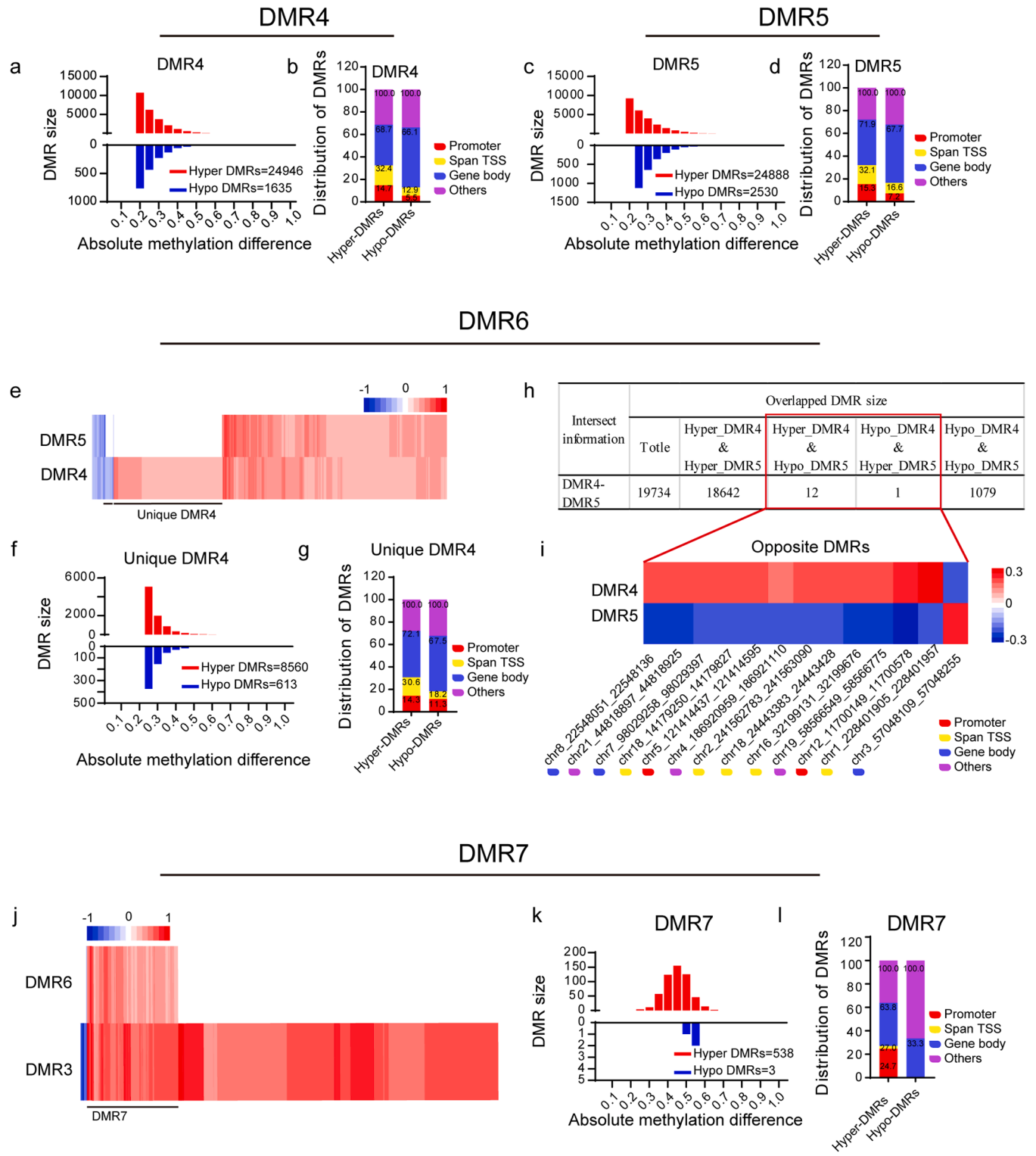

Fig. 3. Characterization of DMR4–DMR7. a DMRs between 18 independent *de novo* samples and five DCAG-induced CR samples. A total of 24 946 hyper-DMRs in *de novo* samples exhibited a decreased methylation level in DCAG-induced CR samples, whereas only 1 635 hypo-DMRs in *de novo* samples exhibited an increased methylation level. **b** Genomic distribution of DMR4. DMRs mapped to promoter regions were predominantly hypermethylated. **c** DMRs between 18 independent *de novo* samples and two CR samples induced by the "7 + 3" standard chemotherapy regimen. A total of 24 888 hyper-DMRs in *de novo* samples exhibited decreased methylation, whereas 2 530 hypo-DMRs exhibited increased methylation. **d** Genomic distribution of DMR5. DMRs mapped to promoter regions were predominantly hypermethylated. **e** Alignment of DMR5 with DMR4. Unique DMR4 regions and overlapping DMRs with opposite change directions were included in DMR6. **f** A total of 9 173 unique DMR4 regions were identified, among which 8 560 and 613 exhibited decreased and increased methylation patterns, respectively. **g** Genomic distribution of unique DMR4 regions. **h** Table presenting 19 734 overlapping DMRs between DMR5 and DMR4. **i** Heatmap illustrating the 13 overlapping DMRs with opposite change directions. **j** Alignment of DMR6 with DMR3. Overlapping DMRs were included in DMR7. **k** DMR7 included 538 hyper-DMRs and three hypo-DMRs. **l** Genomic distribution of DMR7. No hypo-DMR7 regions were mapped to promoter regions, whereas 172 (27.04%) of hypermethylated regions were mapped to promoter regions of 187 genes. DMR, differentially methylated region; DCAG, decitabine, cytarabine, aclarubicin, and G-CSF; CR, complete response.

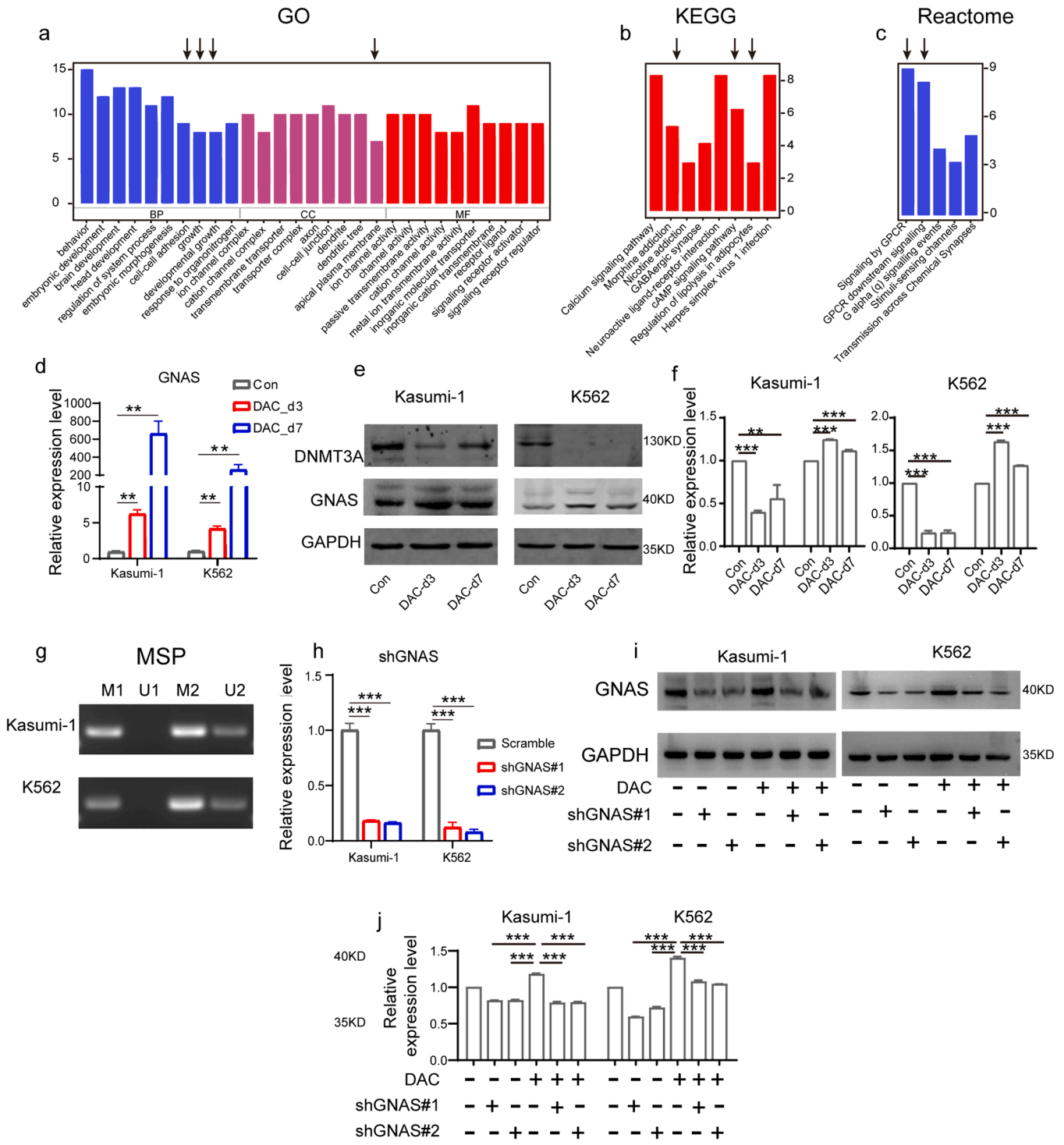

Fig. 4. Identification of DAC-sensitive genes in AML. a–c Gene ontology, Kyoto Encyclopedia of Genes and Genomes, and Reactome enrichment analyses of 187 genes with downregulated methylation in promoter regions after exposure to DAC. Arrows indicate items in which *GNAS* is enriched. **d** Quantitative real-time polymerase chain reaction and **e, f** western blotting analyses showing increased mRNA and protein levels of GNAS and DNMT3A after treatment with 10 nM DAC for three or seven consecutive days. **g** Methylation pattern in Kasumi-1 and K562 cells of the two regions mapped to the *GNAS* promoter. **h** *GNAS* expression analysis after shGNAS transfection. **i, j** Western blot analysis of GNAS levels upon its knockdown by shGNAS lentiviruses. DMR, differentially methylated region; DAC, decitabine. * $p < 0.05$, ** $p < 0.01$, and *** $p < 0.001$.

demethylation effect mainly by downregulating *DNMT*s, the depletion of *DNMT1* is known to be irrelevant to the DAC response rate [20]. Daskalakis et al. [21] showed that decreased methylation of *p15* after DAC treatment is associated with the clinical response in patients with myelodysplastic syndrome. However, neither the baseline methylation status nor the reversal of methylation in *p15* regions were associated with the clinical response to DAC of AML patients [22]. In addition, dynamically methylated tumor suppressor genes, such as *p16, CDH1, DAPK1*, and *SOCS1*, failed to predict the clinical response to DAC [21, 22].

The abovementioned studies were designed to verify the relationship between known hypermethylated genes and clinical responses to DAC.

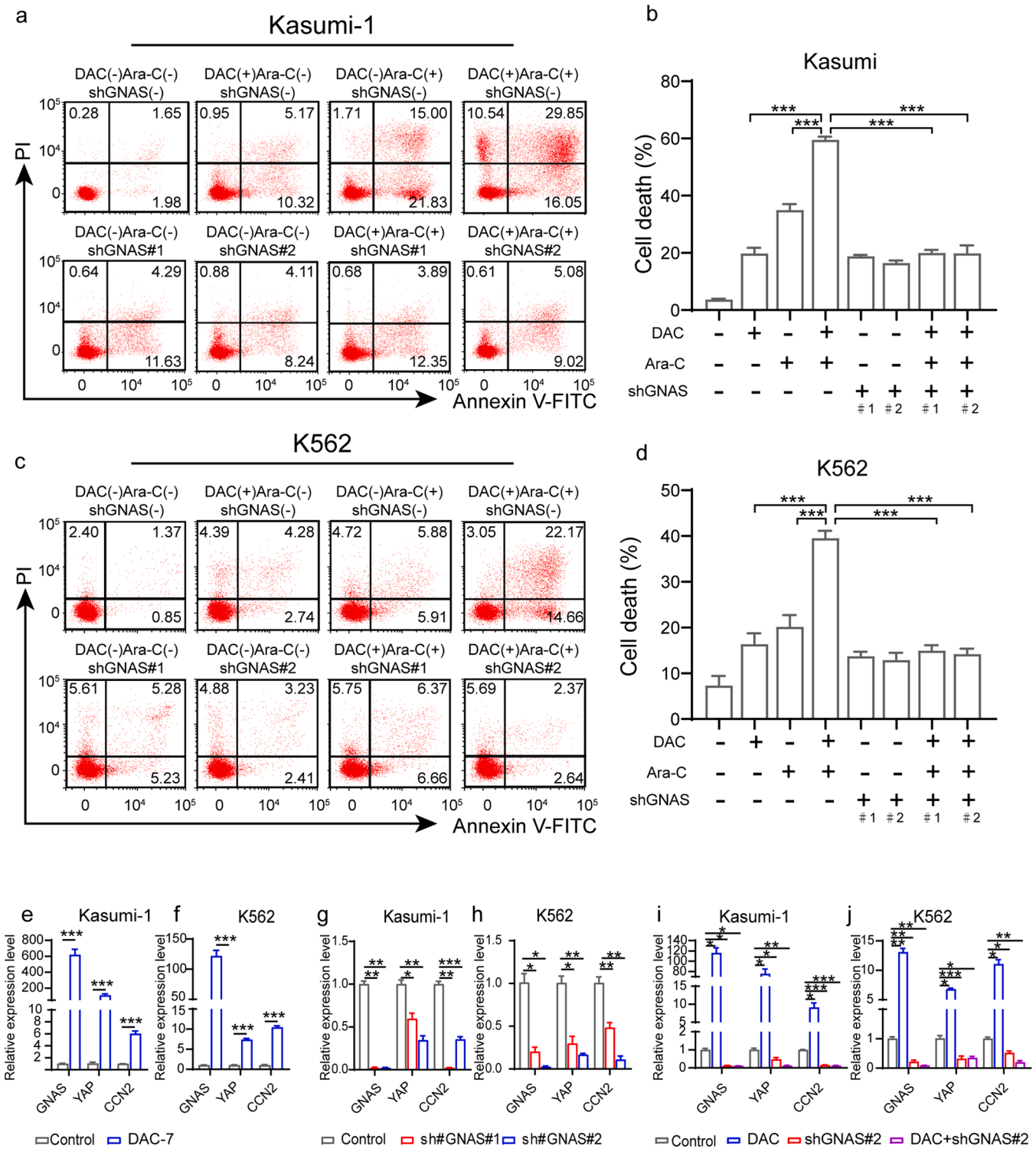

Fig. 5. Molecular events underlying DAC sensitivity in AML. a–d Effects of *GNAS* on apoptosis of Kasumi-1 (a, b) and K562 (c, d) cells. Cells were transfected with shGNAS lentiviruses and treated with 10 nM DAC and 100 nM Ara-C. Cell apoptosis was assayed using Annexin V-FITC/propidium iodide double staining. **e, f** Quantitative real-time polymerase chain reaction (qRT-PCR) analysis of *YAP* and *CCN2* expression in Kasumi-1 (e) and K562 (f) cells upon *GNAS* knockdown. **g** Kasumi-1 and **h** K562 cells were treated with 10 nM DAC for 3 days, transfected with shGNAS lentivirus, or transfected with shGNAS lentivirus and treated with DAC and were then subjected to qRT-PCR to analyze the expression of *GNAS, YAP,* and *CCN2*. DAC, decitabine; Ara-C, cytarabine. * $p < 0.05$, ** $p < 0.01$, and *** $p < 0.001$.

Given the global but selective demethylation effect of DAC on the genome [21–25], an unknown set of genes could contribute for an increased vulnerability to DAC treatment. By analyzing the baseline DNA methylation status using next-generation sequencing in uniformly treated patients with chronic myelomonocytic leukemia who were responsive or resistant to DAC, Meldi et al. [26] identified a set of DMRs that accurately predicted the response to DAC. However, simultaneous analysis of somatic mutations and gene expression did not differentiate

responders from non-responders. In the present study, we investigated DAC-sensitive DMRs in patients with AML by comparing the methylation landscape of CR samples with that of *de novo* samples using MethylC-capture sequencing, a next-generation sequencing technology [27]. Moreover, we identified DAC-responsive DMRs by comparing methylation alterations in paired and unpaired AML samples. The elimination of leukemia blast cells by treatment with either DAC combined or traditional chemotherapy regimen resulted in the restoration of a non-specific methylation landscape by the recovery of normal bone marrow cells. The phenomenon that the size of the DMRs induced by traditional chemotherapy was comparable to that of the DMRs induced by DAC-based combo chemotherapy further supports the restoration of the methylation landscape resultant of bone marrow recovery and emphasizes the importance of removing non-specific DMRs. We eliminated non-specific DMRs induced by the combined DAC regimen by removing alteration-containing regions that overlapped with those induced by the traditional treatment regimen. This analysis approach fine-tuned our selection in to 541 DAC-sensitive DMRs, among which 538 were hypermethylated and three were hypomethylated at baseline. These results indicate that, in addition to inducing demethylation, DAC treatment can drive the methylation pattern of patients with AML prone to normal.

In accordance with a previous study that explored DAC-sensitive methylation markers in chronic myelomonocytic leukemia [26], the genomic locations predominantly affected by DAC treatment were distal to non-promoter regions. Nevertheless, previous studies may have failed to identify predictive markers because they focused on well-known promoter regions. Although various evidences indicate that non-promoter methylation regulation plays a critical role [28], our study also focused on promoter regions since the gain and loss of methylation in these regions frequently affects gene expression, which is technically easy to detect in clinical practice.

According to our functional enrichment analysis, *GNAS* was identified as a candidate gene associated with the response to DAC treatment. Leukemia cells pre-sensitized with DAC are much more vulnerable to exogenous stressors, including cytotoxic drugs [17], cellular therapies [29], and molecular-targeted therapies [30]. We retrospectively evaluated the function of *GNAS* in cells sequentially treated with a combination of DAC and Ara-C. *GNAS* mediates the anti-apoptotic synergistic effect of DAC and Ara-C. Moreover, we demonstrated that *GNAS* inhibition suppresses *YAP* and *CCN2* expression, which were upregulated in DAC-treated cells. These findings may indicate that *GNAS* mediates the antineoplastic activity of DAC potentially via *YAP-CCN2* signaling.

GNAS (G-protein α subunit), a PKA activator, has frequently been associated with the development of pancreatic cancer [31,32], small cell lung cancer [33], and colorectal cancer [34]. *It has been shown that GNAS can function as a proto-oncogene in solid tumors* [35], while in Sonic hedgehog-driven medulloblastomas, *GNAS* served as a tumor suppressor [36]. It appeared that *GNAS* may play different roles in different malignancies. In this study, we found that promoter methylation of *GNAS* served as a prognostic indicator in patients with AML treated with DAC. In accordance with the previous study conducted by Decock A, et al [37], they found that *GNAS* was methylation silenced in neuroblastoma, and methylation of *GNAS* was associated with decreased survival. Yet, in AML, there was no significant correlation between GNAS methylation and survival rates.

Conclusion

In summary, our study identifies *GNAS* as a predictive biomarker for the response to DAC-based therapy in patients with AML; however, these findings warrant further confirmation by *in vivo* studies and clinical assessment. Moreover, an objective cutoff value derived from a large cohort study is needed to better characterize the methylation status of *GNAS* in newly diagnosed patients and establish the prognostic value of *GNAS* in AML. Conclusively, we suggest that hypermethylation of *GNAS* promoter may be indicate of better responses of AML patients to DAC-based treatments.

Ethics declarations

The study protocol for the use of clinical samples was approved by the Ethics Committee of the Chinese People's Liberation Army General Hospital and conducted in accordance with the principles of the Helsinki Declaration. Written informed consent was obtained from all participants prior to specimen collection.

Consent for publication

Not applicable.

Availability of data and materials

We declare that the methylation sequencing data that support the findings of this study, including all the relevant raw data, will be available from the corresponding author upon reasonable request.

Funding

This work was supported by the Chinese National Major Project for New Drug Innovation (2019ZX09201002003), National Natural Science Foundation of China (82270172, 81903635, 82030076, 82070161, 81970151, 81670162, and 81870134), Shenzhen Science and Technology Foundation (RCYX20221008092851074, RCBS20210706092216031, JCYJ20220531103014031, JCYJ20230808104915031, JCYJ20190808163601776, JCYJ20200109113810154), Shenzhen Key Laboratory Foundation (ZDSYS20200811143757022), and Sanming Project of Shenzhen (SZSM202111004), Shenzhen Medical Research Fund (A2303007).

CRediT authorship contribution statement

Shujiao He: Writing – original draft. **Yan Li:** Investigation, Resources. **Lei Wang:** Resources, Validation. **Yisheng Li:** Data curation, Software. **Lu Xu:** Methodology, Validation. **Diya Cai:** Methodology. **Jingfeng Zhou:** Conceptualization, Supervision. **Li Yu:** Conceptualization, Funding acquisition, Writing – review & editing.

Declaration of competing interest

The authors declare that they have no competing interests.

Acknowledgements

We would like to acknowledge the technical support provided by Instrumental Analysis Center of Shenzhen University (Xili Campus).

Supplementary materials

Supplementary material associated with this article can be found, in the online version, at doi:10.1016/j.neo.2024.100965.

References

[1] T.K. Kim, S.D. Gore, A.M. Zeidan, Epigenetic therapy in acute myeloid leukemia: current and future directions, Semin. Hematol. 52 (2015) 172–183.
[2] S. Baylin, T.H. Bestor, Altered methylation patterns in cancer cell genomes: cause or consequence? Cancer Cell 1 (2002) 299–305.
[3] S. Huang, et al., Epigenetic silencing of eyes absent 4 gene by acute myeloid leukemia 1-eight-twenty-one oncoprotein contributes to leukemogenesis in t(8;21) acute myeloid leukemia, Chin. Med. J. (Engl.) 129 (2016) 1355–1362.
[4] A.D. Kelly, et al., Demethylator phenotypes in acute myeloid leukemia, Leukemia 32 (2018) 2178–2188.
[5] Y. Li, et al., A novel epigenetic AML1-ETO/THAP10/miR-383 mini-circuitry contributes to t(8;21) leukaemogenesis, EMBO Mol. Med. 9 (2017) 933–949.

[6] N. Khan, et al., Efficacy of single-agent decitabine in relapsed and refractory acute myeloid leukemia, Leuk. Lymphoma 58 (2017) 1–7.
[7] I. Pusic, et al., Maintenance therapy with decitabine after allogeneic stem cell transplantation for acute myelogenous leukemia and myelodysplastic syndrome, Biol. Blood Marrow Transplant. 21 (2015) 1761–1769.
[8] T. Meyer, et al., Functional characterization of BRCC3 mutations in acute myeloid leukemia with t(8;21)(q22;q22.1), Leukemia 34 (2020) 404–415.
[9] H.M. Kantarjian, et al., Multicenter, randomized, open-label, phase III trial of decitabine versus patient choice, with physician advice, of either supportive care or low-dose cytarabine for the treatment of older patients with newly diagnosed acute myeloid leukemia, J. Clin. Oncol. 30 (2012) 2670–2677.
[10] S.M. Leonard, T. Perry, C.B. Woodman, P. Kearns, Sequential treatment with cytarabine and decitabine has an increased anti-leukemia effect compared to cytarabine alone in xenograft models of childhood acute myeloid leukemia, PLoS ONE 9 (2014) e87475.
[11] J.P. Issa, et al., Phase 1 study of low-dose prolonged exposure schedules of the hypomethylating agent 5-aza-2′-deoxycytidine (decitabine) in hematopoietic malignancies, Blood 103 (2004) 1635–1640.
[12] F. Ferrara, F. Lessi, O. Vitagliano, E. Birkenghi, G. Rossi, Current therapeutic results and treatment options for older patients with relapsed acute myeloid leukemia, Cancers 11 (2019) 224.
[13] W. Xu, et al., Correction to: DNMT3A reads and connects histone H3K36me2 to DNA methylation, Protein Cell 11 (2020) 230.
[14] Y. Li, et al., Detection of prognostic methylation markers by methylC-capture sequencing in acute myeloid leukemia, Oncotarget 8 (2017) 110444–110459.
[15] G. Kunde-Ramamoorthy, et al., Comparison and quantitative verification of mapping algorithms for whole-genome bisulfite sequencing, Nucleic Acids Res. 42 (2014) e43.
[16] F. Juhling, et al., metilene: fast and sensitive calling of differentially methylated regions from bisulfite sequencing data, Genome Res. 26 (2016) 256–262.
[17] T. Qin, et al., Effect of cytarabine and decitabine in combination in human leukemic cell lines, Clin. Cancer Res. 13 (2007) 4225–4232.
[18] P. Feng, et al., Deacetylation of YAP1 promotes the resistance to chemo- and targeted therapy in FLT3-ITD(+) AML cells, Front. Cell Dev. Biol. 10 (2022) 842214.
[19] Q. Cong, et al., A self-amplifying loop of YAP and SHH drives formation and expansion of heterotopic ossification, Sci. Transl. Med. 13 (599) (2021) eabb2233.
[20] W. Blum, et al., Phase I study of decitabine alone or in combination with valproic acid in acute myeloid leukemia, J. Clin. Oncol. 25 (2007) 3884–3891.
[21] M. Daskalakis, et al., Demethylation of a hypermethylated P15/INK4B gene in patients with myelodysplastic syndrome by 5-Aza-2′-deoxycytidine (decitabine) treatment, Blood 100 (2002) 2957–2964.
[22] T.E. Fandy, et al., Early epigenetic changes and DNA damage do not predict clinical response in an overlapping schedule of 5-azacytidine and entinostat in patients with myeloid malignancies, Blood 114 (2009) 2764–2773.
[23] D. Roulois, et al., DNA-demethylating agents target colorectal cancer cells by inducing viral mimicry by endogenous transcripts, Cell 162 (5) (2015) 961–973.
[24] Q. Liang, et al., The novel human endogenous retrovirus-related gene, psiTPTE22-HERV, is silenced by DNA methylation in cancers, Int. J. Cancer 127 (8) (2010) 1833–1843.
[25] F. Wolff, et al., The double-edged sword of (re)expression of genes by hypomethylating agents: from viral mimicry to exploitation as priming agents for targeted immune checkpoint modulation, Cell Commun. Signal. CCS 15 (1) (2017) 13.
[26] K. Meldi, et al., Specific molecular signatures predict decitabine response in chronic myelomonocytic leukemia, J. Clin. Investig. 125 (2015) 1857–1872.
[27] F. Allum, et al., Dissecting features of epigenetic variants underlying cardiometabolic risk using full-resolution epigenome profiling in regulatory elements, Nat. Commun. 10 (2019) 1209.
[28] X. Yang, et al., Gene body methylation can alter gene expression and is a therapeutic target in cancer, Cancer Cell 26 (2014) 577–590.
[29] Y. Wang, et al., Low-dose decitabine priming endows CAR T cells with enhanced and persistent antitumour potential via epigenetic reprogramming, Nat. Commun. 12 (2021) 409.
[30] E. Chang, et al., The combination of FLT3 and DNA methyltransferase inhibition is synergistically cytotoxic to FLT3/ITD acute myeloid leukemia cells, Leukemia 30 (2016) 1025–1032.
[31] K.C. Patra, et al., Mutant GNAS drives pancreatic tumourigenesis by inducing PKA-mediated SIK suppression and reprogramming lipid metabolism, Nat. Cell Biol. 20 (7) (2018) 811–822.
[32] P.E. Hollstein, R.J. Shaw, GNAS shifts metabolism in pancreatic cancer, Nat. Cell Biol. 20 (7) (2018) 740–741.
[33] G.L. Coles, et al., Unbiased proteomic profiling uncovers a targetable GNAS/PKA/PP2A axis in small cell lung cancer stem cells, Cancer Cell 38 (1) (2020) 129–143. e127.
[34] H.A. Afolabi, et al., A GNAS gene mutation's independent expression in the growth of colorectal cancer: a systematic review and meta-analysis, Cancers 14 (22) (2022) 5480.
[35] X. Jin, et al., Elevated expression of GNAS promotes breast cancer cell proliferation and migration via the PI3K/AKT/Snail1/E-cadherin axis, Clin. Transl. Oncol. 21 (9) (2019) 1207–1219, official publication of the Federation of Spanish Oncology Societies and of the National Cancer Institute of Mexico.
[36] X. He, et al., The G protein α subunit Gαs is a tumor suppressor in Sonic hedgehog-driven medulloblastoma, Nat. Med. 20 (9) (2014) 1035–1042.
[37] A. Decock, et al., Genome-wide promoter methylation analysis in neuroblastoma identifies prognostic methylation biomarkers, Genome Biol. 13 (10) (2012) R95.